Electronic Supplementary Information

Free-Supporting Dual-Confined Porous Si@c-ZIF@carbon nanofibers for high-performance lithium-ion batteries

Jiale Chen[†], Xingmei Guo[†], Mingyue Gao, Jing Wang, Shangqing Sun, Kai Xue, Shuya Zhang,Yuanjun Liu, Junhao Zhang*

[a]School of Environmental and Chemical Engineering, Jiangsu University of Science and Technology, Zhenjiang, Jiangsu 212003, China

[b]School of the Environment and Safety Engineering, Jiangsu University, Zhenjiang, Jiangsu, 212013, China

Corresponding author: Junhao Zhang; E-mail: jhzhang6@just.edu.cn

Experimental section

Chemicals

Analytical zinc nitrate hexahydrate ($Zn(NO_3)_2·6H_2O$), methanol (MeOH), and dimethylformamide (DMF) were purchased from Sinopharm Chemical Reagent Co., LTD. 2-methylimidazole (2-mim) and Polyvinylpyrrolidone (PVP, Mw = 58000) were bought from Aladdin Technologies Inc. (Shanghai, China). Silicon nanoparticles (Si NPs ~120 nm) were purchased from Shanghai Nai Ou nanomaterials technology Co., LTD.

Synthesis of Si@ZIF-8

Si nanoparticles (0.15 g) was ultrasonic dispersed in 50 mL of ethanol containing 0.8 g PVP. After being stirred for 10 h, the solution was centrifuged to obtain Si@PVP intermediate. The obtained Si@PVP was dispersed into a 2-methylimidazole solution (1.97 g 2-mim in 60 mL methanol) to obtain solution A. 1.638 g $Zn(NO_3)_2·6H_2O$ was dissolved in 60 mL methanol to form solution B. Then, Solution B was added into solution A with stirring 24 h. Finally, the mixed solution was washed methanol for three times and oven-dried at 60 °C overnight to obtain Si@ZIF-

8 core-shell structure. ZIF-8 precursor without Si nanoparticles was prepared for comparison.

Synthesis of Si@ZIF-8@PAN precursor and Si@c-ZIF@CNFs

Si@ZIF-8@PAN precursor was prepared via electrospinning process. Firstly, 0.4 g Si@ZIF were fully dispersed in 5 mL of DMF under ultrasonic treatment. Then, 0.45 g PAN was added into the solution with stirring at 60 °C overnight to obtain the electrospinning colloidal solution. The obtained solution was loaded into a 5 mL syringe with a 21-gauge needle. The high-voltage applied between the needle tip and collector wrapped by an aluminum foil was maintained at 18 kV. The distance between the needle tip and the collector was 12 cm. The injection speed was fixed at a flow rate of 0.5 mL h^{-1}. Finally, the fibers on aluminum foil was oven-dried at 80 °C overnight to obtain Si@ZIF-8@PAN precursor. Si@PAN was prepared by electrospinning Si nanoparticles and PAN under the same conditions.

Si@c-ZIF@CNFs was obtained by carbonizing Si@ZIF-8@PAN precursor. The Si@ZIF-8@PAN peeled off from aluminum foil was sandwiched between alumina plates. Subsequently, they were pre-oxidized at 260 °C in air for 3 h and then carbonized at 800 °C for 3 h in argon flow with a ramp rate of 5 °C min^{-1} to obtain Si@c-ZIF@CNFs. Additionally, Si@c-ZIF, Si@CNFs and c-ZIF were prepared under the same carbonization conditions for comparison.

Materials characterization

The morphologies of the samples was investigated by field emission scanning electron microscopy (FESEM, ZEISS Merlin Compact). The interior structure and elemental distribution of samples were observed by high resolution transmission electron microscopy (HRTEM, JEM 2100F) and corresponding energy-dispersive X-ray (EDX). The crystal structure and composition of the samples were characterized by X-ray diffractometer (XRD, Shimadzu XRD-6000, Cu Kα radiation with 2θ range from 10° to 80°) and Raman spectrometer. The surface chemical composition and element valence of Si@c-ZIF@CNFs were detected using X-ray photoelectron spectroscopy (XPS, AXIS UltraDLD). N_2 adsorption and desorption isotherms were

investigated by Micromeritics ASAP 2020 at 77 K.

Electrochemical measurement

The electrochemical performances of self-supporting flexible Si@c-ZIF@CNFs composite was investigated by assembling R2032 coin-type half cells. The Si@c-ZIF@CNFs film was cut into round pieces with a diameter of 13 mm as self-supporting anode, and the mass is about 1.0 $mg \cdot cm^{-2}$. The lithium metal and Celgard 2400 polypropylene membrane were used as the counter electrode and separator, respectively. The electrolyte is 1.0 $mol \cdot L^{-1}$ $LiPF_6$ dissolved in a mixture solvent of ethylene carbonate (EC) and diethyl carbonate (DEC) (1:1, v/v). Si@CNFs can also be used directly as electrode material for comparison, and the mass is about 1.0 $mg \cdot cm^{-2}$. For Si nanoparticles and Si@c-ZIF composites, the electrodes were prepared by stirring the mixture of active materials, acetylene black and carboxymethyl cellulose (7:1.5:1.5 in weight) in deionized water overnight. Copper foil coated with the obtained slurry is oven-dried at 80 °C for 12 h. The mass loadings of Si nanoparticles and Si@c-ZIF are 0.8~1.0 $mg \cdot cm^{-2}$.

Galvanostatic discharge/charge profiles and rate capacity of the half-cells were recorded in the range of 0.01 to 3.0 V by using LAND CT2001A. The cyclic voltammetry (CV) curves were conducted on an electrochemical workstation (CHI760E) at a scan rate of 0.1 mV s^{-1}. The electrochemical impedance spectra (EIS) were recorded in a frequency range of 10^5 Hz to 10^{-2} Hz.

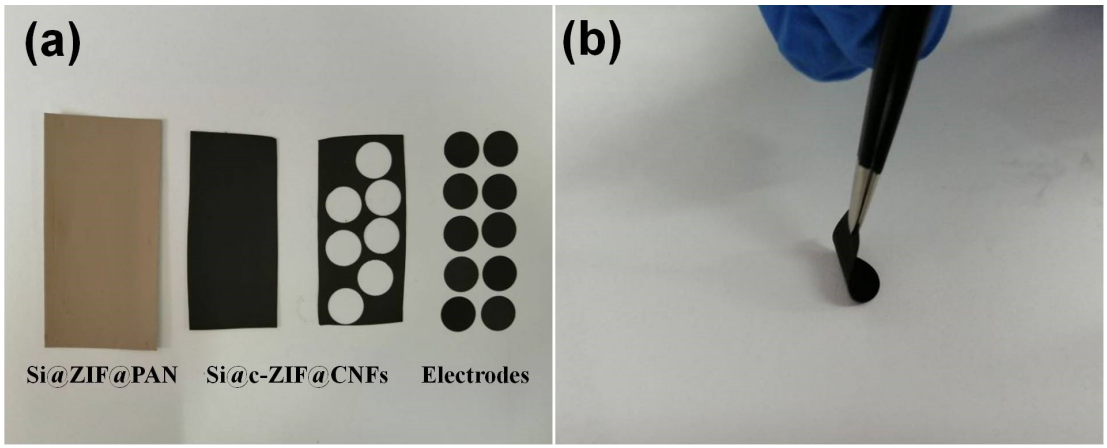

Fig. S1 (a) Digital photograph of Si@ZIF@PAN precursor, Si@c-ZIF@CNFs nanofiber paper and self-supporting electrodes; (b) Digital photograph of Si@c-ZIF@CNFs electrode.

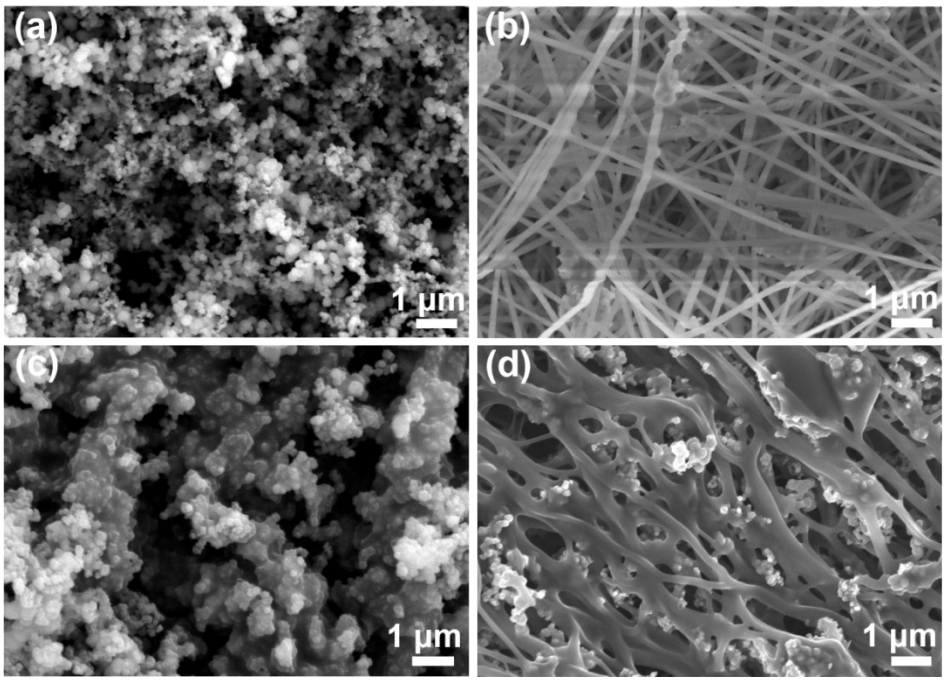

Fig. S2 FESEM images of (a) Silicon nanoparticles, (b) Si@PAN, (c) Si@c-ZIF and (d) Si@CNF.

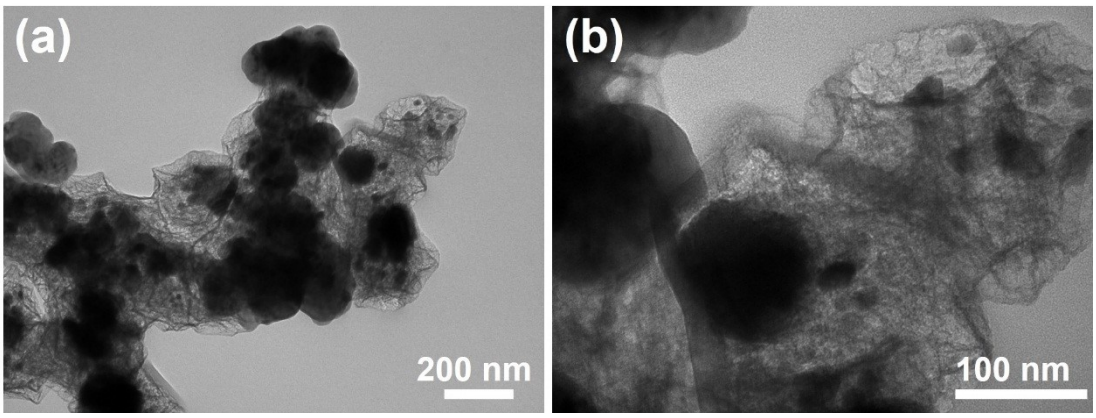

Fig. S3 (a) and (b) TEM images of Si@c-ZIF.

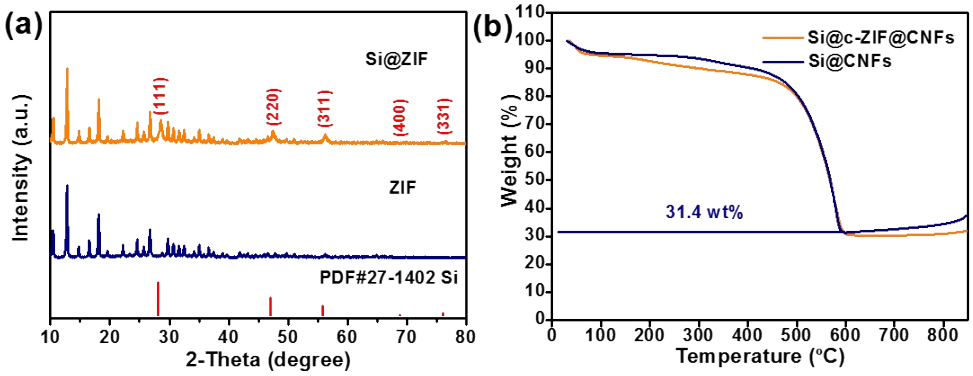

Fig. S4 (a) XRD patterns of Si@ZIF and ZIF; (b) TG curves of Si@c-ZIF@CNFs and Si@CNFs.

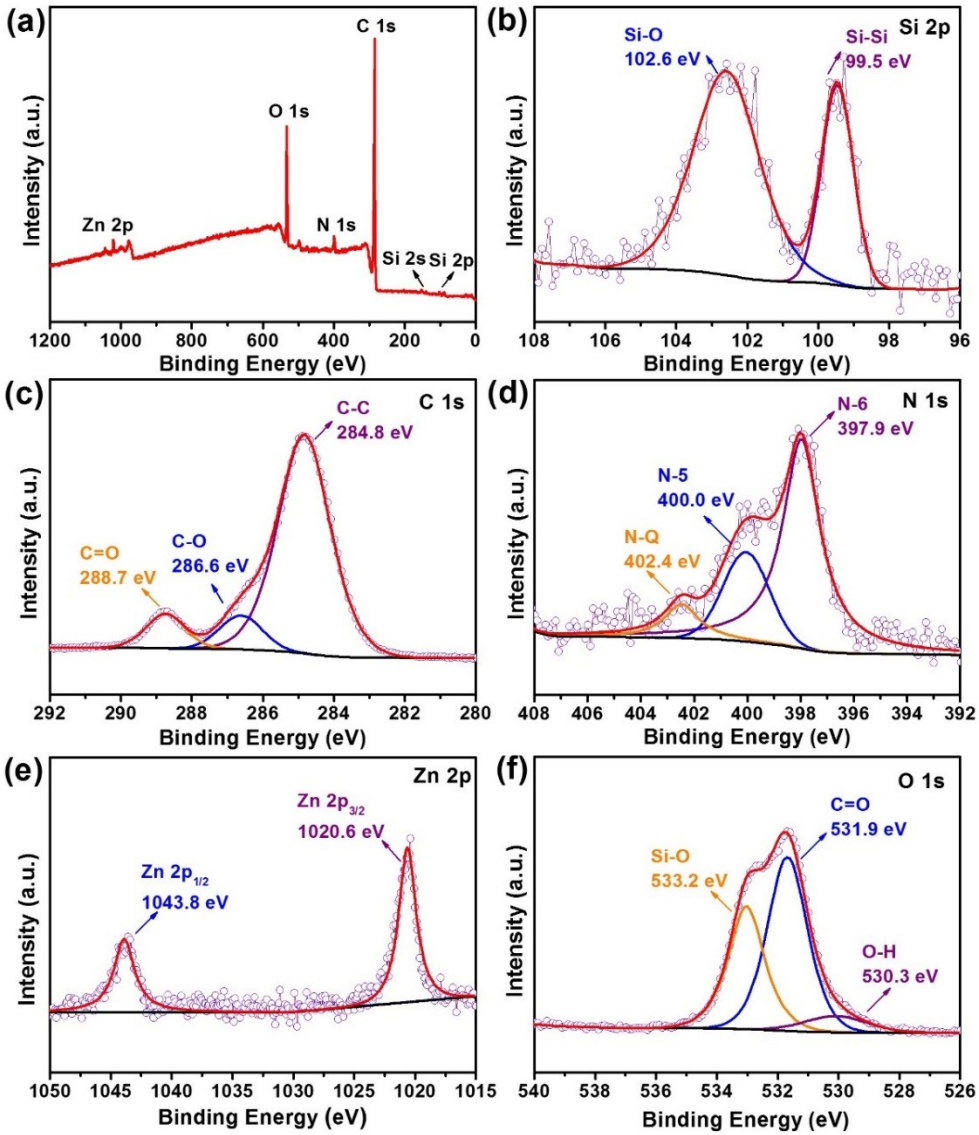

Fig. S5 XPS spectra of Si@c-ZIF@CNFs: (a) XPS survey spectrum; High resolution spectra of (b) Si 2p, (c) C 1s, (d) N 1s, (e) Zn 2p and (f) O 1s.

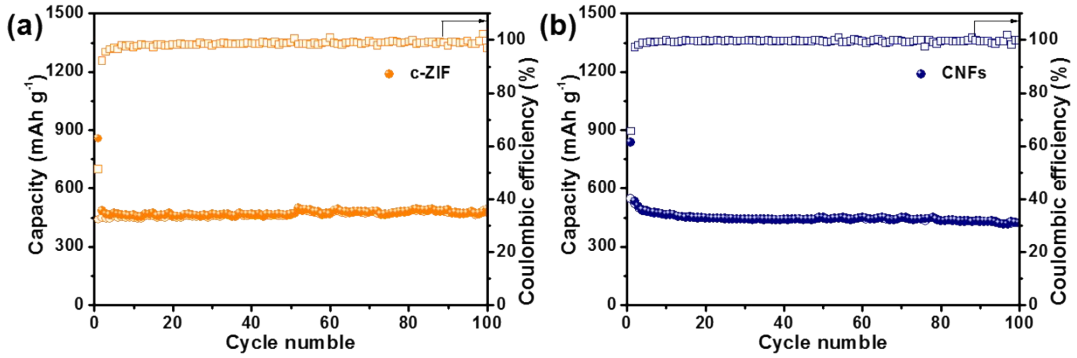

Fig. S6 Cycling performances of c-ZIF (a) and CNFs (b) at 2 A g^{-1} for 100 cycles.

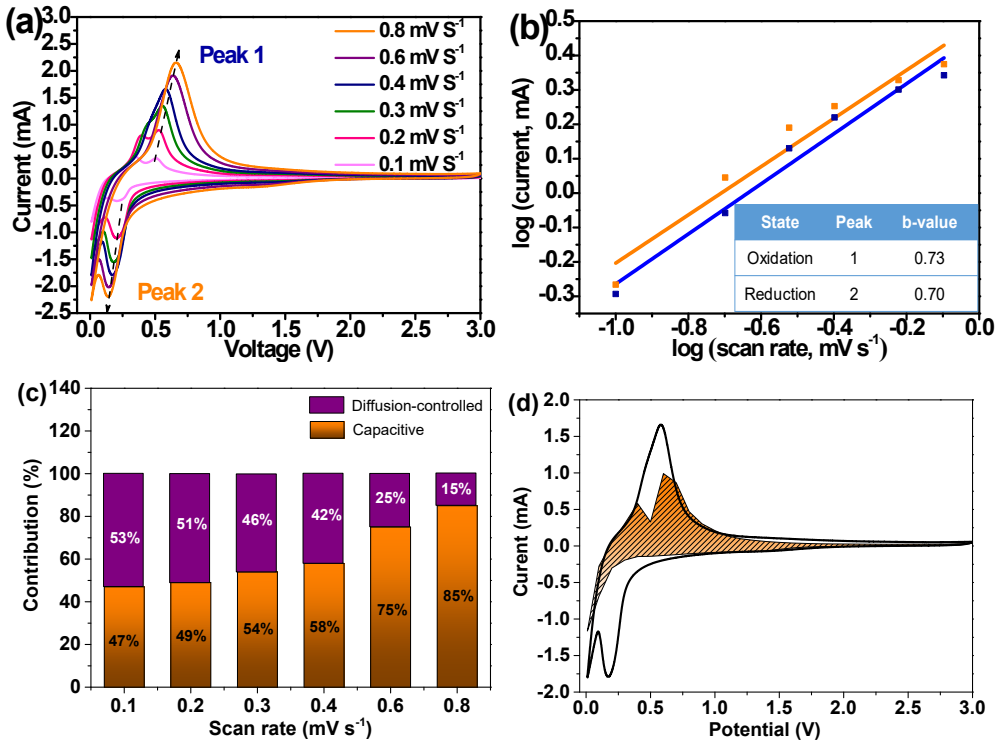

Fig. S7 (a) CV curves at different scanning rates of the Si@c-ZIF@CNFs; (b) the linear relationship of log(*i*) against log(*v*) and the insert shows b-values; (c) Contribution ratio of the capacitive and diffusion-controlled charges at different scan

rates; (d) Capacitive contribution to the total current contribution at 0.4 $mV \cdot s^{-1}$.

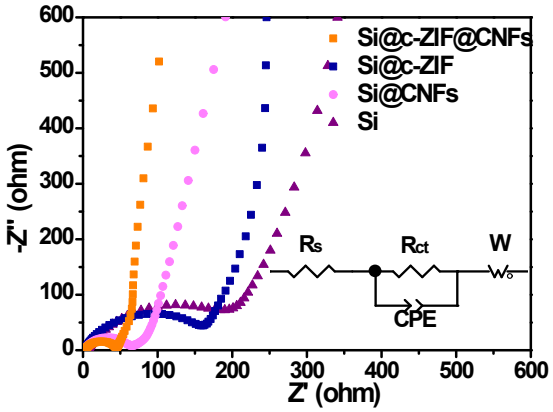

Fig. S8 EIS of Si@c-ZIF@CNFs, Si@c-ZIF, Si@CNFs and pure Si nanoparticles.

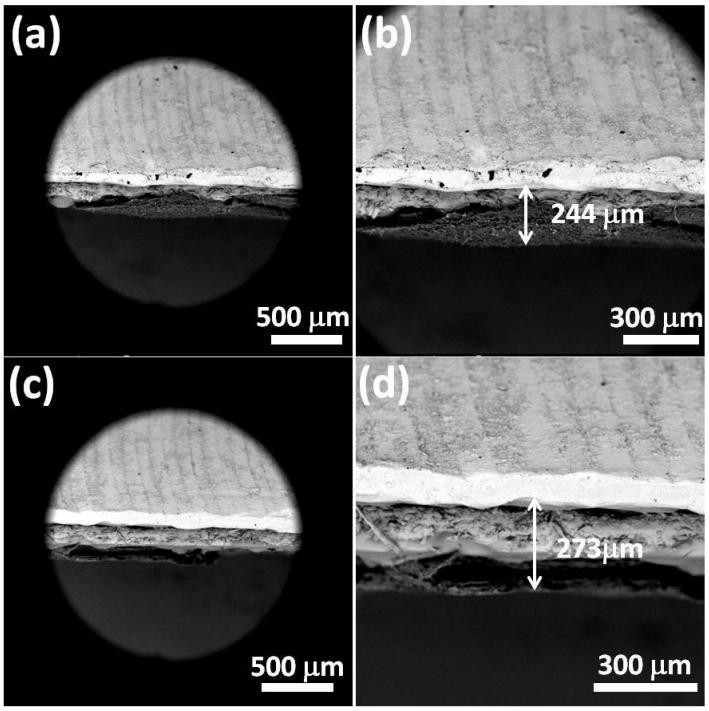

Fig. S9 SEM images of Si@c-ZIF@CNFs membrane: (a) and (b) fresh; (c) and (d) after 500 cycles.

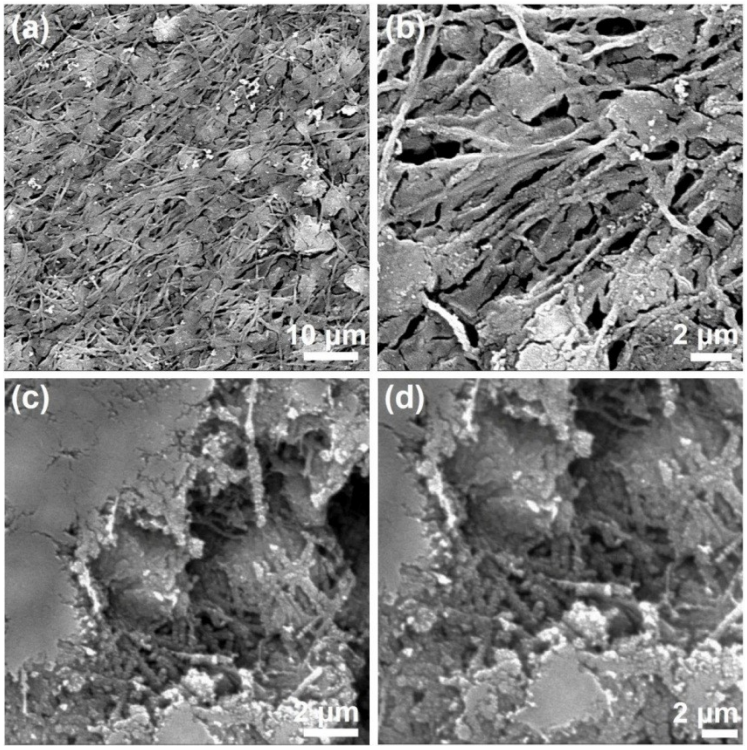

Fig. S10 SEM images of (a) and (b) Si@c-ZIF@CNFs after 100 cycles at 0.2 A g^{-1}; (c) and (d) Si@c-ZIF@CNFs after 1000 cycles at 1 A g^{-1}.

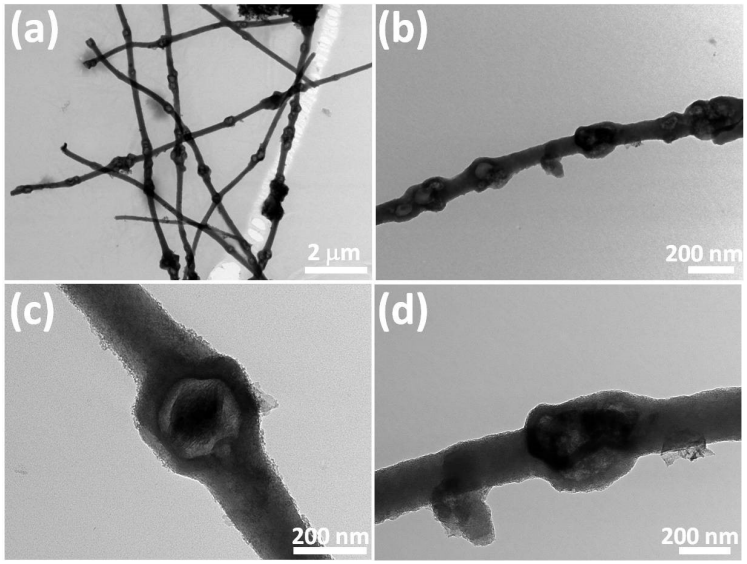

Fig. S11 TEM images of Si@c-ZIF@CNFs as self-supporting anode for lithium-ion battery after 1000 cycles at 1 A g^{-1}.

Table S1 Specific surface area and porous information of different samples.

Samples	Specific surface area ($m^2 g^{-1}$)	Total pore volume ($cm^3 g^{-1}$)	Mean pore diameter (nm)
Si@c-ZIF@CNFs	320.89	0.3419	4.2620
Si@c-ZIF	625.90	0.4288	2.7405
Si@CNFs	182.76	0.1598	3.4979

Table S2 The cycling stability and rate ability of various Si/C-based anodes.

Sample	Initial CE (%)	Current density ($A g^{-1}$)	Cycle number	Final capacity ($mA h g^{-1}$)	Current density ($A g^{-1}$)	Capacity ($mA h g^{-1}$)	Refs
Si@c-ZIF@CNFs	**77.0**	1.0	1000	518.6	5.0	523.9	**This work**
MP-Si NPs/C spheres	34.6	0.2	100	581	1.0	421	1
Si NPs/C nanofibre	44.5	1.0	200	547	12.8	467	2
Si NPs/graphene	54.0	0.4	1300	668	2	307	3
Si/Cu/GR	71.3	0.2	100	647	2	393	4
Si/C	78.1	0.3	100	611.3	4	480.3	5
Porous Si/C	69.0	0.5	100	732.1	1	437.2	6
Carbon double modified Si	89.0	0.4	300	874	5 C	380	7
Pumpkin-like Si/C	73	0.5	500	538.6	5	437.4	8
Graphene-scaffolded Si/graphite	75.6	0.075	100	503.1	2.25	310	9
Bowl-like Si/rGO	90.8	0.1	100	450	1.0	100	10
Hierarchical Si/C	80.7	2.0	1000	684	4.0	430	11
Porous Si/rGO	74.9	1.0	150	580	3.0	345	12

rGO/Si film	50.4	0.2	200	713	1.0	433	13
Porous 3D G/Si/G sandwich	~	0.5	194	300	0.6	360	14
3-APTS-EGO/Si@C	66.5	0.4	450	774	2.0	310	15
H-Si@N-C@rGO	54.2	0.2	100	818	5.0	461	16
Nano-Si/G sheets	62.4	0.2	300	645	5.0	475	17
Flexible Si/G	62.0	0.5	100	560	2.0	370	18
Nano-Si/N-C/G porous foam	66.3	0.4	400	812	3.2	541	19
Si/MWCNT/G	~	0.2	500	695	5.0	120	20

Refereneces

1. T. Shen, X.H. Xia, D. Xie, Z.J. Yao, Y. Zhong, J.Y. Zhan, D.H. Wang, J.B. Wu, X.L. Wang and J.P. Tu, *J. Mater. Chem. A*, 2017, **5**, 11197.

2. S. Fang, L.F. Shen, Z.K. Tong, H. Zheng, F. Zhang and X.G. Zhang, *Nanoscale*, 2015, **7**, 7409.

3. Z.P. Luo, Q.Z. Xiao, G.T. Lei, Z.H. Li and C.J. Tang, *Carbon*, 2016, **98**, 373.

4. T.J. Xu, N. Lin, W.L. Cai, Z. Yi, J. Zhou, Y. Han, Y.C. Zhu and Y.T. Qian, I*norg. Chem. Front.*, 2018, **5**, 1463.

5. R. Zhou, H. Guo, Y. Yang, Z. Wang, X. Li and Y. Zhou, *J. Alloys Compd.*, 2016, **689**, 130.

6. Z. Zhang, Y. Wang, W. Wen, Q. Tan, Y. Chen, H. Li, Z. Zhong and F. Su, *Angew. Chem. Int. Ed.*, 2014, **53**, 5165.

7. Y. Yang, Z. Lu, J. Xia, Y. Liu, K. Wang and X. Wang, *Chem. Eng. Sci.*, 2021, **229**, 116054.

8. Y. Zeng, Y. Huang, N. Liu, X. Wang, Y. Zhang, Y. Guo, H.H. Wu, H. Chen, X. Tang and Q. Zhang, *J. Energy Chem.*, 2021, **54**, 727.

9. S.S. Zhu , J.B. Zhou , Y. Guan , W.L. Cai , Y.Y. Zhao , Y.C. Zhu , L.Q. Zhu , Y.C. Zhu and Y.T. Qian, *Small*, 2018, **14**, 1802457 .

10. Z. Zhang, Y. Du and H. Li, *Nanotechnology*, 2019, **31**, 095402.

11. X.Y. Yue, Z. Yan, Y. Song, X.J. Wu and Y.N. Zhou, *Nanoscale*, 2018, **10**, 19195.

12. M.S. Wang, Z.Q. Wang, R. Jia, Y. Yang, F.Y. Zhu, Z.L. Yang, Y. Huang, X. Li and W. Xu, *Appl. Surf. Sci.*, 2018, **456**, 379.

13. X. Cai, W. Liu, Z. Zhao, S. Li, S. Yang, S. Zhang, Q. Gao, X. Yu, H. Wang and Y. Fang, *ACS Appl. Mater. Interfaces*, 2019, **11**, 3897.

14. Z. Feng, C. Huang, A. Fu, L. Chen, F. Pei, Y. He, X. Fang, B. Qu, X. Chen, A.M. Ng and J. Cui, *Thin Solid Films*, 2020, **693**, 137702.

15. X. Li, X. Tian, T. Yang, W. Wang, Y. Song, Q. Guo and Z. Liu, *J. Power Sources*, 2018, **385**, 84.

16. B.D. Assresahegn, B.D. Ossonon and D. Belanger, *J. Power Sources*, 2018, **391**, 41.

17. W. Sun, R. Hu, M. Zhang, J. Liu and M. Zhu, *J. Power Sources*, 2016, **318**, 113.

18. H. Huang, R. Chen, S. Yang, W. Zhang, Y. Fang, L. Li, Y. Liu and J. Huang, *Synth. Met.*, 2019, **247**, 212.

19. D. He, X. Huang and M. Li, *Carbon*, 2019, **141**, 531.

20. G. Hatipoglu, M. Alaf and H. Akbulut, *J. Mater. Sci. Mater. Electron.*, 2019, *30*, 2067.